Towards a near quantum-limited planar SLUG amplifier at microwave frequencies

Gemma Chapman, Jamie Potter, Laith Meti, Olena Shaforost, Ed Romans, John Gallop, Ling Hao

***Abstract*—The Superconducting Low-inductance Undulatory Galvonometer (SLUG) microwave amplifier is distinct from a conventional SQUID amplifier in that the signal to be amplified is directly injected into the SQUID loop, allowing high frequency operation. Here, we discuss a planar SLUG amplifier constructed with nanobridge weak-links fabricated from a single niobium layer. DC characterisation of the SLUG gain element is presented for two nanobridge fabrication techniques. Measurements show that junctions fabricated from Ne focused-ion-beam, and from 100 keV electron-beam lithography, have significantly different DC characteristics with critical currents on the order of 100 µA and 1 mA respectively. Both variants exhibit maximum forward transfer functions greater than 1.5 mV/Φ_0, which is larger than those reported in Nb SIS-junction SLUGs. Theoretical modelling has shown that an amplifier containing a planar, nanobridge SLUG as a gain element is expected to exhibit gain exceeding 15 dB with large instantaneous bandwidth, and can be designed to operate well in excess of 20 GHz.**

***Index Terms*—Low-noise amplifier, Superconducting low-inductance undulatory galvonometer (SLUG), Nanobridge, Electron-beam lithography (EBL), Focused-ion-beam (FIB)**

I. Introduction

THE RAPID development in recent years of cryogenic low-noise amplifiers has been driven by the equally rapid progress in superconducting quantum technologies, and the requirement to read out extremely low-power signals with minimal added noise. As well as widespread application in quantum information processing, these amplifiers are also enabling technologies in the fields of cosmology and fundamental physics. Haloscope experiments seek to detect the axion as a dark matter candidate, through the detection of virtual microwave photons arising from the decay of the hypothetical axion in a strong magnetic field [1]. The axion mass is theorised to be proportional to the photon frequency, and contemporary experiments will be tuned to operate in the 4–10 GHz range. A separate family of proposed experiments intend to determine the absolute mass of the electron neutrino, using Cyclotron Radiation Emission Spectroscopy (CRES) [2], [3]. In this paradigm, spectroscopy is performed on electrons emitted during the beta-decay of atomic tritium, by trapping them in a region of strong magnetic field, inducing cyclotron radiation. The endpoint of the electron energy spectrum, corresponding to a radiation frequency of 27 GHz in a 1 T field [4], is then precisely measured. Both experiments are only made possible with a highly sensitive microwave receiver operating at the appropriate frequency.

Amplifiers based on the Superconducting QUantum Interference Device (SQUID) are attractive due to the low noise properties of the SQUID — a SQUID amplifier can in theory achieve noise performance approaching the standard quantum limit (SQL) of $\hbar/2$ [5]. A linear, phase preserving amplifier has a minimum noise temperature of $T_Q = hf/k_B \approx 50$ mK at 1 GHz [6]. The Microstrip Superconducting Amplifier (MSA) is an archetypal SQUID amplifier, and was developed for axion haloscope experiments [7]. The signal input to the dc SQUID is via an inductive coil, which sits above the SQUID loop forming a microstrip resonator. It has successfully achieved a noise temperature of $\sim 2T_Q$ [8] but its microstrip configuration produces a geometric-based negative gain - frequency relationship producing a practical upper frequency limit of 1 GHz [9]. Mention is also given here to parametric amplifiers which can operate with added noise at, and even below the SQL [10], [11], [12], [13]. Whilst these have unsurpassed noise performance, SQUID-based amplifiers may still provide advantages due to their broader bandwidths, larger dynamic range and simpler circuitry requirements.

The Superconducting Low-inductance Undulatory Galvanometer (SLUG) amplifier is a variant of the dc SQUID amplifier, where the signal is injected directly into the SQUID loop as a current, rather than inductively coupled by a flux transformer, thus allowing efficient coupling of GHz signals at the amplifier input [14]. The SLUG amplifier is also advantageous over MSA-style amplifiers as it can be readily modelled due to the low inductance geometry and the easy resolution of the SLUG modes from the input matching network.

Hover et al. developed a SLUG amplifier where a pair of Nb/Al−AlO_x−Al/Nb SIS junctions define a SQUID loop within microstrip optimised for qubit readout with a gain of 19 dB at 6.6 GHz with a 50 MHz bandwidth [15], [16]. Here we present an alternative approach to the SLUG amplifier, utilising nanobridge Josephson elements, where the SLUG loop is formed from a single niobium layer — greatly simplifying the fabrication process. Nanobridges provide low noise performance [17], [18], and are inherently suitable for high frequency operation due to their large critical current density and negligible capacitance. Indeed, we have previously

Gemma Chapman, Jamie Potter (corresponding author: jamie.potter@npl.co.uk), Laith Meti, Olena Shaforost, John Gallop and Ling Hao are with the National Physical Laboratory, Teddington, TW11 0LW, UK. Ed Romans is with the London Centre for Nanotechnology, UCL, 17-19 Gordon Street, London WC1H 0AH, UK

The authors would like to thank the UK Science and Technology Facilities Council (STFC) for funding this work through support for the Quantum Sensors for the Hidden Sector (QSHS) and Quantum Technologies for Neutrino Mass (QTNM) collaborations under grants ST/T006064/1 and ST/T006137/1. Further acknowledgement and thanks are given to the National Metrology Institute, Beijing, China for providing the niobium films.

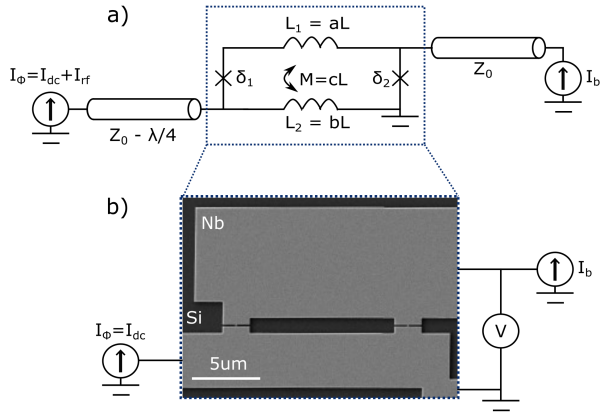

Fig. 1. a) Circuit model for the SLUG amplifier. δ_i is the phase across the Josephson junctions, L is the loop inductance, where a, b and c are numerical constants and M is the mutual inductance. I_b is the dc bias current, and I_Φ is the input signal, which contains a dc component for flux-biasing, and the rf signal to be amplified. The signal is input via a quarter-wave transformer with characteristic impedance Z_0. b) A scanning electron microscope image of a fabricated SLUG element, as represented by the circuit model inside the blue dashed box. The dc measurement circuit is overlaid.

reported nanobridge SQUIDs operating above 50 GHz [19], and nanoSQUIDs exhibiting flux noise of $0.2\,\mu\Phi_0/\mathrm{Hz}^{1/2}$ at 6.8 K [20]. In addition, nanobridges are highly resilient to magnetic fields, compared with their SIS counterparts, which is a desirable property given the high magnetic fields involved in haloscope and CRES experiments.

In this study, we investigate the feasibility of a planar SLUG amplifier, through a combination of dc characterisation of the SLUG gain element and numerical circuit modelling. We have produced SLUGs with nanobridges fabricated by electron-beam lithography (EBL) and focused-ion-beam (FIB), and measured them at $T = 3.8$ K up to T_c with the purpose of comparing their relative suitability. From here, we model the expected gain and noise of a fully realised planar nanobridge SLUG amplifier at frequencies up to 27 GHz and consider potential routes towards future device optimisation.

II. Fabrication

In order to investigate the SLUG gain element and inform the design of a fully matched SLUG amplifier, we fabricated and characterised the dc response of an isolated nanobridge SLUG. Fig. 1a) shows the circuit diagram of a SLUG amplifier, where the blue boxes outline the SLUG gain element and a scanning electron microscope image of a typical device, which is fabricated from a 150 nm-thick film of niobium sputtered onto a thermally oxidised silicon substrate.

A nanobridge Josephson junction is formed of a short, narrow constriction in a superconducting material, where the length and width of the constriction should be comparable with the Ginzburg-Landau coherence length $\xi(T)$. In niobium film, $\xi(4.2\,\mathrm{K}) \approx 40$ nm [21]. Nanobridges of the required dimensions can be fabricated with standard nanofabrication techniques [22]. In the present work, we fabricated equivalent sets of isolated SLUG devices using two techniques: EBL and neon FIB milling. The large features of the circuit are patterned by 100 keV EBL, and then transferred into the Nb film by reactive-ion etching using CHF_3 and SF_6. The process then branches depending on the nanobridge fabrication method. For the devices with EBL-fabricated nanobridges, patterning of the SLUG loop and nanobridges is performed in a single exposure. The resulting nanobridges have lengths of 130–140 nm and widths of 40–55 nm. For the devices with FIB-fabricated nanobridges, the EBL pattern is written with micron-scale 'precursor' nanowires, which are subsequently reduced in size by 20 keV Ne FIB milling to dimensions of 60 nm long by 40–45 nm wide.

III. Results

We have measured the output voltage of the SLUG, as illustrated in Fig. 1, as a function of dc current applied either across the junctions (I_b), or across the flux line (I_Φ). The $V(I_b)$ and $V(I_\Phi)$ curves of two typical SLUG devices are shown in Fig. 2. The devices in question have equivalent geometries outside of the nanobridges. The EBL SLUG shows critical current I_0 values $\mathcal{O}(1\,\mathrm{mA})$ between 7.25–8.25 K and exhibits thermal hysteresis [23], [24] in the $V(I_b)$ curve below 7 K, limiting the operating regime. In comparison, the FIB SLUG has I_0 values $\mathcal{O}(100\,\mu\mathrm{A})$ at 4–5 K and still maintains non-hysteric behaviour at 4 K. The difference in operating temperature is also illustrated by the SLUGs' $R(T)$ curves (Fig.2ii) insets). The EBL SLUG shows a single, sharp transition at $T = 8.8$ K, matching the critical temperature T_c of the Nb film. In contrast, the FIB SLUG shows the sharp transition of the film followed by a gradual progression to the onset of superconductivity within the nanobridges at $T_c = 5.5$ K. The nanobridge normal state resistance R can be extracted from $V(I_b)$ graphs above I_0. The EBL nanobridges have $R = 1.4 \pm 0.1\,\Omega$ compared to the FIB nanobridge $R = 12 \pm 1\,\Omega$, despite their bridge lengths being twice as long. This is likely due to the Ne ions used in the FIB milling process implanting within and damaging the Nb and underlying substrate, suppressing T_c and I_0, and increasing the resistivity of the Nb. These are known side-effects of FIB fabrication [25], [26], however further work is required to understand the ion beam's effect on the superconducting state.

The lower panels of Fig.2 show the $V(I_\Phi)$ of the SLUGs. We observe that both graphs are similar to the $V(\Phi)$ of a dc SQUID, apart from a shift in the flux bias due to the inductive asymmetry of the SLUG loop. From the measured period ΔI_Φ, we can extract the SLUG loop inductance simply by $(b-c)L = \Phi_0/\Delta I_\Phi$. We find $(b-c)L = 2.42 \pm 0.02$ pH for the EBL SLUG and $(b-c)L = 2.12 \pm 0.02$ pH for the FIB SLUG. Given their identical loop geometries, the difference in $(b-c)L$ between the devices is unexpected. It is thought that this could be due to the variation in the nanobridge geometry or that the FIB damage reduces the kinetic inductance of the nanobridge. 3D-MSLI, a software that calculates the inductances of superconducting circuits [27] predicted a loop inductance $L = 7.61$ pH and $(b-c) = 0.23$, giving $(b-c)L = 1.75$ pH for this SLUG loop geometry which is about 17 % smaller than the experimentally obtained inductance. This discrepancy is likely due to the simplified model

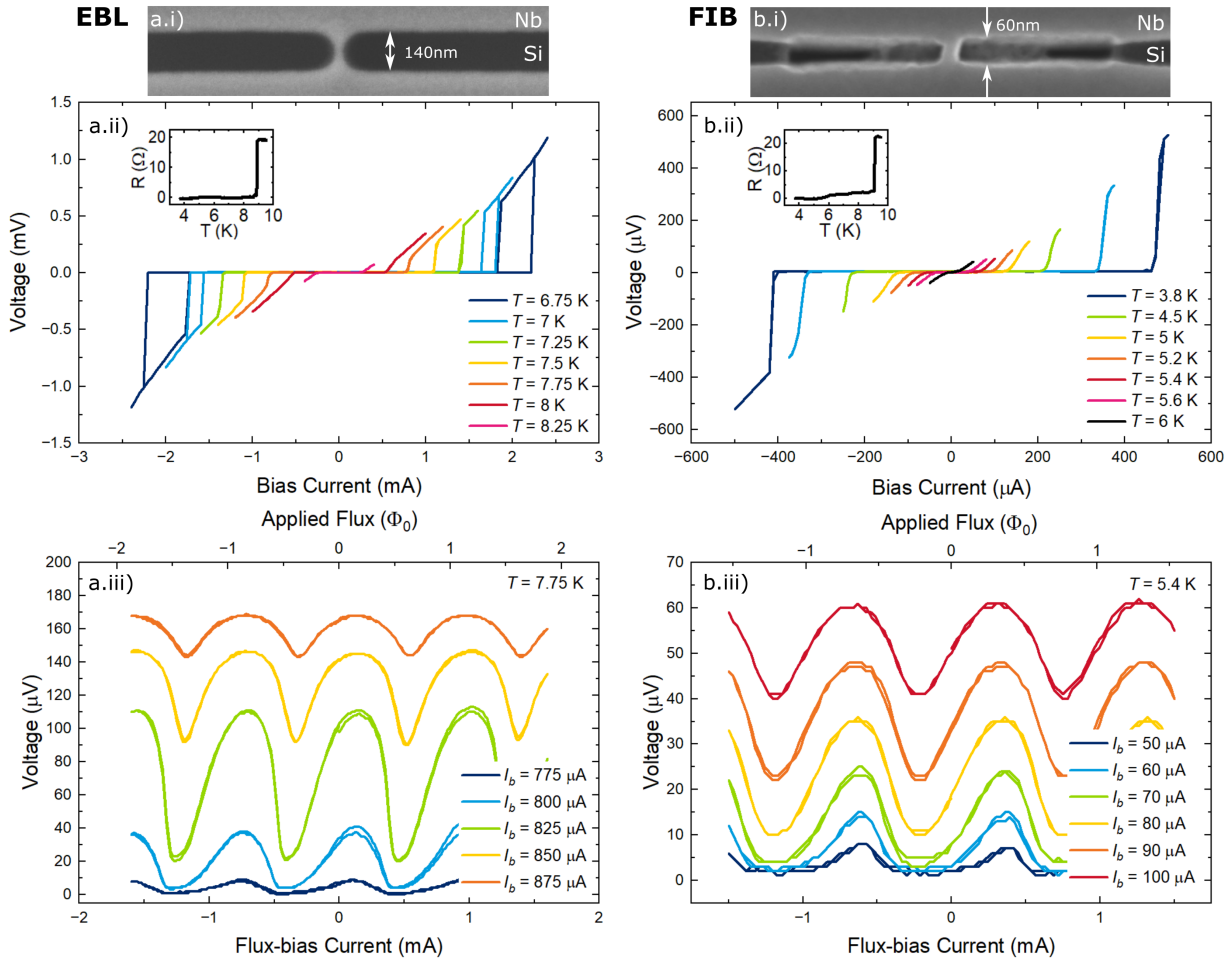

Fig. 2. DC characteristics of identical SLUGs with a) EBL and b) FIB nanobridges. (i) Scanning electron microscope images of a single nanobridge. ii) $V(I_b)$ curves across a range of temperatures. The inset in each shows $R(T)$ of the SLUG. iii) $V(I_\Phi)$ curves for a range of bias currents at a fixed temperature.

neglecting the measurement leads, which we suspect induces a more complicated current distribution around the SLUG loop.

Lastly from the measured $V(I_\Phi)$ curves, we can find the transfer function $V_\Phi = \partial V/\partial\Phi$ values for our SLUGs, where we distinguish between the rising (V_Φ^+) and the falling (V_Φ^-) slope, due to the skew of the curves. We hypothesize that this skew can be attributed to asymmetric nanobridge junctions from similar observations of skewed $V(I_\Phi)$ curves in gated graphene Josephson junctions [28] and high-T_c dc SQUIDs with asymmetric junctions [29]. The transfer function is a measure of the sensitivity of the SLUG to a changing magnetic flux, and directly relates to the gain of the SLUG amplifier. It is noted here that the skew of the $V(I_\Phi)$ curve could be considered advantageous as it may increase V_Φ^+ at the cost of V_Φ^-, or vice-versa. For the EBL SLUGs, we find $V_\Phi^+ = 0.86\,\mathrm{mV}/\Phi_0$ and $V_\Phi^- = -0.26\,\mathrm{mV}/\Phi_0$. For the FIB SLUGs, $V_\Phi^+ = 0.08\,\mathrm{mV}/\Phi_0$ and $V_\Phi^- = -0.13\,\mathrm{mV}/\Phi_0$. Across the full set of SLUGs measured, maximum V_Φ values of $1.67\,\mathrm{mV}/\Phi_0$ and $2.75\,\mathrm{mV}/\Phi_0$ were found from EBL and FIB SLUGs respectively. Published V_Φ values for SLUGs with SIS Josephson junctions [15] are $\mathcal{O}(0.1\,\mathrm{mV}/\Phi_0)$, which suggests that our planar, nanobridge SLUGs are a promising candidate for the gain element within a high-gain amplifier.

IV. Numerical Modelling

Complementary to the development of their SLUG amplifier [15], Ribeill et al. produced a comprehensive theoretical toolbox which can be used to model, among other things, the frequency-dependent gain and noise of a SLUG amplifier. Here, we employ and adapt this toolbox, combined with our dc characterisation results, to simulate the gain and noise properties of a planar, nanobridge SLUG amplifier.

A brief description of the method and key equations are replicated below, but for full details we direct the reader to [14]. First we write down the coupled equations of motion for the gauge-invariant phase-difference across the pair of nanobridges $\delta_{1,2}$ in a SLUG

$$\dot{\delta}_1 = \frac{1}{\pi\beta_L}\Big((\delta_2-\delta_1) - 2\pi\phi_{dc}\Big) - \sin\delta_1 - (b-c)i_{rf} + v_{n,1} \tag{1}$$

$$\dot{\delta}_2 = i_b - \frac{1}{\pi\beta_L}\Big((\delta_2-\delta_1) - 2\pi\phi_{dc}\Big) - (1-\alpha)\sin\delta_2 + (b-c)i_{rf} + v_{n,2}. \tag{2}$$

The lower case notation denotes the use of dimensionless units, defined as follows: $i \equiv I/I_0$, $v \equiv V/I_0R$, $\phi \equiv \Phi/\Phi_0$,

where I_0 is the critical current and R is the normal state resistance of a single nanobridge. β_L is the screening parameter $\beta_L = 2I_0L/\Phi_0$, α is a junction asymmetry parameter, defined such that $I_2 = (1-\alpha)I_1$, and $v_{n,i}$ is a noise voltage. The dimensionless parameters a, b, c describe the distribution of inductance around the SLUG loop, as shown in Fig.1.

Equations 1 and 2 are numerically integrated using a 4$^{\text{th}}$ order Runge-Kutta solver to give the time-dependent voltage across the SLUG. The maximum power gain, G_m, of the SLUG gain element, when assumed to be sitting within a perfectly matched environment, is given by

$$G_m = \frac{1}{4\rho_i\rho_o}\left(\frac{V_\Phi}{\omega}\right)^2 \tag{3}$$

where we have defined the dimensionless impedance parameters $\rho_i = R_i \cdot R/(\omega L)^2$ and $\rho_o = R_o/R$. $R_{i,o}$ is the real part of the input and output impedance respectively. It can be seen that a primary contributor to the gain is the forward transfer function, V_Φ, with a negative quadratic dependency on the microwave signal frequency ω. The gain of the SLUG amplifier can then be calculated by modelling the gain element as a variable impedance terminating a $\lambda/4$ resonator.

In Fig. 3b), the frequency-dependent gain for SLUG amplifiers simulated with our typical nanobridge dc parameters (detailed in the Fig. caption), and a simple planar loop geometry (example in Fig. 3a)), are shown. In each case the loop geometry is chosen to ensure $\beta_L \approx 1$. Two curves are displayed for each nanobridge type, where the devices are coupled to a resonator with $Z_0 = 2\,\Omega$ and bare resonant frequency of $f_0 = 8\,\text{GHz}$ or $f_0 = 28\,\text{GHz}$.

For these example amplifiers, simulations show gain approaching 20 dB with a −3 dB bandwidth of 400 MHz between 5–10 GHz, and 15 dB gain with −3 dB bandwidth of 1.5 GHz above 20 GHz. Inductive loading from the SLUG element reduces the operating frequency of the amplifier from the bare resonator frequency. This loading increases at higher frequencies, and the bandwidth of the amplifier can be seen to broaden. Between the two nanobridge types, the FIB devices produce higher gain, which may be explained by their larger I_0R product. However, due to the larger loop inductance, the amplifier sees a larger negative frequency shift.

The amplifier noise, in terms of added photons at the signal frequency, n, is shown in Fig. 3c). In order to model this we have assumed that the experimental temperature is low, and therefore the quantum noise dominates over Johnson noise. It can be seen that the frequency of maximum gain is not equal to the frequency of minimum noise, as the optimal input matching impedance for gain and noise are not the same [14]. It is possible in general to find a good compromise between gain and noise — in the case of the lower frequency FIB SLUG, at 6 GHz we find a gain of 15 dB and added noise within a factor of 4 of the standard quantum limit.

From this set of modelling tools, we can identify a number of considerations for designing a SLUG amplifier which is optimised for a particular application. In order to maximise gain, β_L should be approximately equal to 1. Since I_0 will be dependent on the nanobridge fabrication choices, L can be tuned by varying its length. We note that a smaller loop inductance is beneficial for higher frequency operation. As seen in equations 1 and 2, the strength of coupling of a signal into the loop is scaled by $b - c$, and therefore the geometry of the loop should be designed to maximise this factor, for example by introducing an asymmetry between the upper and lower arms. One should also choose an appropriate input matching impedance to favour high gain or low noise, or find a balance between the two.

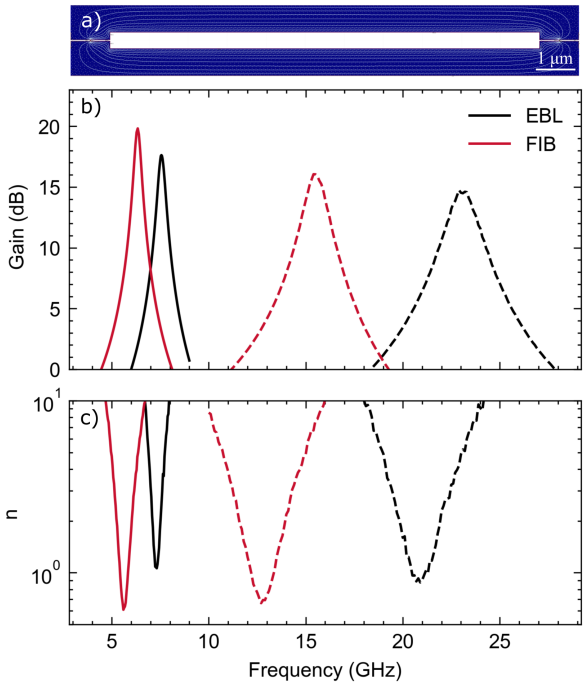

Fig. 3. a) A representative planar SLUG geometry simulated by 3D-MSLI, b) gain and c) noise, in added photons n, for SLUG amplifiers with $a = 1$, $b = 1$ and $c = 0.5$. Gain curves are shown for amplifiers simulated with junction parameters representing EBL ($I_0 = 1\,\text{mA}$ and $R = 1.5\,\Omega$) and FIB ($I_0 = 200\,\mu\text{A}$ and $R = 12\,\Omega$) fabricated nanobridges. Respective loop inductances of $L = 1\,\text{pH}$ and $L = 5\,\text{pH}$ were chosen to give $\beta_L = 0.97$. SLUGs were simulated with input resonators with $f_0 = 8\,\text{GHz}$ (solid lines) and $f_0 = 28\,\text{GHz}$ (dashed lines).

V. Conclusions

We have presented dc characterisation of nanobridge SLUGs, where those nanobridges have been fabricated by both electron-beam lithography, and Ne focused-ion-beam milling. Both EBL and FIB SLUGs show remarkably high flux-to-voltage transfer functions, suggesting their suitability as the gain element in a microwave amplifier. We propose that there is room for both fabrication techniques; the FIB nanobridges operate more readily at lower temperatures, whilst the higher critical currents found in EBL nanobridges make them ideal for higher operating frequencies. A set of numerical modelling tools have been presented that should allow a circuit designer to tailor a SLUG amplifier for the desired application. We simulated a SLUG amplifier based on our typical planar nanobridge SLUG, and found regions with gain approaching 20 dB at frequencies below 10 GHz, and in excess of 15 dB at frequencies above 20 GHz.

REFERENCES

[1] P. Sikivie, "Experimental tests of the "invisible" axion," *Physical Review Letters*, vol. 51, no. 16, pp. 1415–1417, 1983.

[2] B. Monreal and J. A. Formaggio, "Relativistic cyclotron radiation detection of tritium decay electrons as a new technique for measuring the neutrino mass," *Physical Review D*, vol. 80, no. 5, p. 051301, 2009.

[3] A. A. Esfahani, S. Böser, N. Buzinsky, M. C. Carmona-Benitez, C. Claessens, L. De Viveiros, and ..., "The Project 8 Neutrino Mass Experiment," *arXiv preprint arXiv:2203.07349*, 2022.

[4] A. A. Esfahani, V. Bansal, S. Böser, N. Buzinsky, R. Cervantes, C. Claessens, and ..., "Electron radiated power in cyclotron radiation emission spectroscopy experiments," *Physical Review C*, vol. 99, no. 5, p. 055501, 2019.

[5] R. H. Koch, D. J. Van Harlingen, and J. Clarke, "Quantum noise theory for the dc SQUID," *Applied Physics Letters*, vol. 38, no. 5, pp. 380–382, 1981.

[6] C. M. Caves, "Quantum limits on noise in linear amplifiers," *Physical Review D*, vol. 26, no. 8, pp. 1817–1839, 1982.

[7] M. Mück, M. O. André, J. Clarke, J. Gail, and C. Heiden, "Radio-frequency amplifier based on a niobium dc superconducting quantum interference device with microstrip input coupling," *Applied Physics Letters*, vol. 72, no. 22, pp. 2885–2887, 1998.

[8] M. Mück, J. B. Kycia, and J. Clarke, "Superconducting quantum interference device as a near-quantum-limited amplifier at 0.5 GHz," *Applied Physics Letters*, vol. 78, no. 7, pp. 967–969, 2001.

[9] M. Mück, C. Welzel, and J. Clarke, "Superconducting quantum interference device amplifiers at gigahertz frequencies," *Applied Physics Letters*, vol. 82, no. 19, pp. 3266–3268, 2003.

[10] J. Aumentado, "Superconducting parametric amplifiers: The state of the art in Josephson parametric amplifiers," *IEEE microwave magazine*, vol. 21, no. 8, pp. 45–59, 2020.

[11] M. A. Castellanos-Beltran and K. W. Lehnert, "Widely tunable parametric amplifier based on a superconducting quantum interference device array resonator," *Applied Physics Letters*, vol. 91, no. 8, 2007.

[12] T. Yamamoto, K. Inomata, M. Watanabe, K. Matsuba, T. Miyazaki, W. D. Oliver, Y. Nakamura, and J. S. Tsai, "Flux-driven Josephson parametric amplifier," *Applied Physics Letters*, vol. 93, no. 4, 2008.

[13] K. O'Brien, C. Macklin, I. Siddiqi, and X. Zhang, "Resonant phase matching of josephson junction traveling wave parametric amplifiers," *Physical Review Letters*, vol. 113, no. 15, p. 157001, 2014.

[14] G. J. Ribeill, D. Hover, Y. F. Chen, S. Zhu, and R. McDermott, "Superconducting low-inductance undulatory galvanometer microwave amplifier: Theory," *Journal of Applied Physics*, vol. 110, no. 10, 2011.

[15] D. Hover, Y. F. Chen, G. J. Ribeill, S. Zhu, S. Sendelbach, and R. McDermott, "Superconducting low-inductance undulatory galvanometer microwave amplifier," *Applied Physics Letters*, vol. 100, no. 6, 2012.

[16] D. Hover, S. Zhu, T. Thorbeck, G. J. Ribeill, D. Sank, J. Kelly, R. Barends, J. M. Martinis, and R. McDermott, "High fidelity qubit readout with the superconducting low-inductance undulatory galvanometer microwave amplifier," *Applied Physics Letters*, vol. 104, no. 15, 2014.

[17] G. C. Tettamanzi, C. I. Pakes, S. K. Lam, and S. Prawer, "Flux noise in ion-implanted nanoSQUIDs," *Superconductor Science and Technology*, vol. 22, no. 6, p. 064006, 2009.

[18] C. Granata, A. Vettoliere, M. Russo, and B. Ruggiero, "Noise theory of dc nano-SQUIDs based on Dayem nanobridges," *Physical Review B - Condensed Matter and Materials Physics*, vol. 84, no. 22, p. 224516, 2011.

[19] E. Polychroniou, J. Gallop, T. Godfrey, D. Cox, G. Long, J. Chen, E. Romans, and L. Hao, "Investigation of NanoSQUIDs Fabricated with a Range of Focused Ion Beam Sources," *Journal of Physics: Conference Series*, vol. 1559, no. 1, 2020.

[20] L. Hao, J. C. MacFarlane, J. C. Gallop, D. Cox, J. Beyer, D. Drung, and T. Schurig, "Measurement and noise performance of nano-superconducting-quantum- interference devices fabricated by focused ion beam," *Applied Physics Letters*, vol. 92, no. 19, 2008.

[21] E. E. Mitchell and S. K. Lam, "Niobium dc SQUIDs with nanobridge junctions," *Physics Procedia*, vol. 36, pp. 382–387, 2012.

[22] C. Granata and A. Vettoliere, "Nano Superconducting Quantum Interference device: A powerful tool for nanoscale investigations," *Physics Reports*, vol. 614, pp. 1–69, 2016.

[23] S. K. Lam, "Noise properties of SQUIDs made from nanobridges," *Superconductor Science and Technology*, vol. 19, no. 9, p. 963, 2006.

[24] A. Blois, S. Rozhko, L. Hao, J. C. Gallop, and E. J. Romans, "Proximity effect bilayer nano superconducting quantum interference devices for millikelvin magnetometry," *Journal of Applied Physics*, vol. 114, no. 23, 2013.

[25] R. Livengood, S. Tan, Y. Greenzweig, J. Notte, and S. McVey, "Subsurface damage from helium ions as a function of dose, beam energy, and dose rate," *Journal of Vacuum Science Technology B: Microelectronics and Nanometer Structures Processing, Measurement, and Phenomena*, vol. 27, no. 6, pp. 3244–3249, 2009.

[26] A. G. Troeman, H. Derking, B. Borger, J. Pleikies, D. Veldhuis, and H. Hilgenkamp, "NanoSQUIDs based on niobium constrictions," *Nano Letters*, vol. 7, no. 7, pp. 2152–2156, 2007.

[27] M. M. Khapaev, M. Y. Kupriyanov, E. Goldobin, and M. Siegel, "Current distribution simulation for superconducting multi-layered structures," *Superconductor Science and Technology*, vol. 16, no. 1, p. 24, 2002.

[28] M. D. Thompson, M. Ben Shalom, A. K. Geim, A. J. Matthews, J. White, Z. Melhem, Y. A. Pashkin, R. P. Haley, and J. R. Prance, "Graphene-based tunable SQUIDs," *Applied Physics Letters*, vol. 110, no. 16, 2017.

[29] J. Müller, S. Weiss, R. Gross, R. Kleiner, and D. Koelle, "Voltage-flux-characteristics of asymmetric dc SQUIDs," *IEEE Transactions on Applied Superconductivity*, vol. 11, no. 1 I, pp. 912–915, 2001.